Traffano-Schiffo, MV.; Castro Giraldez, M.; Fito Suñer, PJ.; Santagapita, P. (2017). Encapsulation of lactase in Ca(II)-alginate beads: Effect of stabilizers and drying methods. Food Research International. 100(1):296-303. https://doi.org/10.1016/j.foodres.2017.07.020

Accepted Manuscript

Encapsulation of lactase in Ca(II)-alginate beads: Effect of stabilizers and drying methods

Maria Victoria Traffano-Schiffo, Marta Castro-Giraldez, Pedro J. Fito, Patricio R. Santagapita

PII: S0963-9969(17)30341-1
DOI: doi: 10.1016/j.foodres.2017.07.020
Reference: FRIN 6817

To appear in: *Food Research International*

Received date: 12 April 2017
Revised date: 4 July 2017
Accepted date: 6 July 2017

Please cite this article as: Maria Victoria Traffano-Schiffo, Marta Castro-Giraldez, Pedro J. Fito, Patricio R. Santagapita , Encapsulation of lactase in Ca(II)-alginate beads: Effect of stabilizers and drying methods, *Food Research International* (2017), doi: 10.1016/j.foodres.2017.07.020

ENCAPSULATION OF LACTASE IN Ca(II)-ALGINATE BEADS: EFFECT OF STABILIZERS AND DRYING METHODS

Maria Victoria Traffano-Schiffo[a], Marta Castro-Giraldez[a], Pedro J. Fito[a], Patricio R. Santagapita[b,c,*]

[a]Instituto Universitario de Ingeniería de Alimentos para el Desarrollo, Universidad Politécnica de Valencia, Camino de Vera s/n, 46022 Valencia, Spain.

[b]Universidad de Buenos Aires. Facultad de Ciencias Exactas y Naturales. Departamentos de Industrias y Química Orgánica. Buenos Aires, Argentina.

[c]CONICET-Universidad de Buenos Aires. Instituto de Tecnología de Alimentos y Procesos Químicos (ITAPROQ).Buenos Aires, Argentina.

*Corresponding author: prs@di.fcen.uba.ar

ABSTRACT

The purpose of the present work was to analyze the effect of trehalose, arabic and guar gums on the preservation of β-galactosidase activity in freeze-dried and vacuum dried Ca(II)-alginate beads. Freezing process was also studied as a first step of freeze-drying. Trehalose was critical for β-galactosidase conservation, and guar gum as a second excipient showed the highest conservation effect (close to 95%). Systems with T_g values ~ 40 ºC which were stables at ambient temperature were obtained, being trehalose the main responsible of the formation of an amorphous matrix. Vacuum dried beads showed smaller size (with Feret´s diameter below 1.08 ± 0.09 mm), higher circularity (reaching 0.78 ± 0.06) and large cracks in their surface than freeze-dried beads, which were more spongy and voluminous. Ice crystallization of the beads revealed that the crystallization of Ca(II)-alginate system follows the

Avrami kinetics of nucleation and growth. Particularly, Ca(II)-alginate showed an Avrami index of 2.03 ± 0.07, which means that crystal growing is bidimensional. Neither the addition of trehalose nor gums affected the dimension of the ice growing or its rate. These results open an opportunity in the development of new lactic products able to be consumed by lactose intolerance people.

Keywords: hydrogels, β-galactosidase, stability, freeze-drying, vacuum drying, microstructure.

1. Introduction

Lactose is a disaccharide that is found in milk, composed of galactose and glucose covalently bound by a β-galactoside linkage. Most of adult western Europeans can consume milk, however nowadays more and more people are suffering lactose intolerance condition. Lactose intolerance is a condition in which people's ability to digest lactose is decreased, due to insufficiency or lack of the enzyme called β-galactosidase (lactase) in the small intestines, which is crucial to break lactose down into its monosaccharides, suffering several digestive syndromes (Heaney, 2013; Misselwitz et al., 2013). People who suffer this alteration should consume lactose free products or include the enzyme as a supplement (Zhang, Zhang, & McClements, 2017; Estevinho, Ramos, & Rocha, 2015). However, lactase cannot be consumed in its free form due to its instability against to thermal, chemical and mechanical effects, so it, the encapsulation of the enzyme in biopolymers matrices (Wahba, 2016) could not only maintain its catalytic activity but also opens the possibility of its incorporation and consumption inside different foods (Wu et al., 2013).

Sodium alginate is a biopolymer widely used in encapsulation due to its gelation properties in presence of cations such as Ca^{2+}. The gelation occurs due to the exchange of Na^{+} ions from the carboxylic acids of the guluronate (G) blocks with Ca^{2+} ions from the crosslinking solution (Zhang, Zhang, Zou, & McClements, 2016). The G-block of one chain then form junctions with the G-block of the adjacent polymer chain, obtaining the characteristic egg-box structure forming rod-type structures (Zeeb, Saberi, Weiss, & McClements, 2015; Lee, & Mooney, 2012). A recently study performed by negative-staining electron microscopy has revealed that

mannunorate (M) residues also interact in the structure giving flexibility and allowing a greater interaction of G-blocks (He, Liu, Li, & Li, 2016).

Although Ca(II)-alginate beads are easy to perform by the dropping method, are non-toxic, low cost and eco-friendly (Tsai, Chiang, Kitamura, Kokawa, & Islam, 2017; Aguirre Calvo, Busch, & Santagapita, 2017), it shows disadvantages, such as low mechanical strength and low resistance to conservation treatments such as freeze-drying and vacuum-drying (Santagapita, Mazzobre, & Buera, 2012). Therefore, the encapsulation of labile structures in dehydrated or frozen systems is generally carried out in presence disaccharides such as trehalose (Santagapita et al., 2012). Trehalose is a non-reducing disaccharide with protectants properties against dehydration treatments, and lactase was successfully immobilized in trehalose matrix (Santagapita & Buera, 2008b). As was described by Mazzobre, Longinotti, Corti, and Buera (2002), the cryoprotectant effect of the trehalose can be attributed to promote the formation of glassy systems, avoiding deteriorative reactions. It should be taking into account that trehalose interacts with OH-rich biomolecules by hydrogen bonds, stabilizing the structure during thermal and drying treatments. Finally, the addition of others excipients (as natural occurring gums) can improve the stabilizing character of the system (Vasile, Romero, Judis, & Mazzobre, 2016), due to the changes in viscosity and/or interfacial properties, especially relevant for emulsions and suspensions.

Lactase was previously encapsulated in Ca(II)-alginate in presence of secondary excipients (Traffano-Schiffo, Aguirre Calvo, Castro-Giraldez, Fito, & Santagapita, 2017). Trehalose was critical for activity preservation towards freezing and thawing treatments, being improved in guar gum-containing systems. Guar gum increased the

onset temperatures of ice melting (T_m') determined by DSC in Ca(II)-alginate beads containing trehalose. However, this parameter nor the T_g were adequate predictors of the enzyme recovery in beads. On the other hand, it is known that the main factors that affect the stability of the enzyme during freezing process are the crystalline solid fraction obtained, the nucleation and size of the crystals, and the rate of crystallization, which were not analyzed in the previous work. Thus, Johnson-Mehl-Avrami-Kolmogorov (JMAK) model represents a suitable tool to obtain and understand these parameters. Its applicability has been previously demonstrated for lactic acid (De Santis, Pantani, & Titomanlio, 2011), fats (Furlán, Baracco, Lecot, Zaritzky, & Campderrós, 2017) and sugars (Mazzobre, Aguilera, & Buera, 2003).

Finally, considering that wet beads have short stability and the high cost of conservation at freezing temperatures, it is critical to study the dehydration of the beads to achieve long-term stability and conservation even at ambient temperature. Then, the aim of this research was to enhance the stability of lactase against freeze-drying and vacuum drying by its encapsulation in Ca(II)-alginate beads and using trehalose, arabic and guar gums as excipients. Freezing was also studied as a first step of freeze-drying, including isothermal LF-NMR analysis, modeling the kinetics of crystallization.

2. Material and methods

2.1. Materials

The materials used for beads preparation were: sodium alginate (Algogel 5540) from Cargill S.A. (San Isidro, Buenos Aires, Argentina) with a molecular weight of

$1.97 \cdot 10^5$ g/mol and mannuronate/guluronate ratio of 0.6; D-trehalose dihydrate (Hayashibara Co., Ltd., Shimoishii, Okayama, Japan/Cargill Inc., Mineapolis, Minnesota, USA) molecular weight of 378 g/mol; arabic gum (Biopack, Zárate, Buenos Aires, Argentina) molecular weight of 250.000 g/mol and a purity of 99%; guar gum (Cordis S.A., Villa Luzuriaga, Buenos Aires, Argentina) molecular weight of 220.000 g/mol and a mannose/galactose ratio of 1.8 and β-galactosidase from *Aspergillus Oryzae* (8.0 U/mg) (Sigma-Aldrich Co, Ltd, Saint Louis, USA). One enzymatic unit was defined as the amount of enzyme able to hydrolyze 1.0 μmol of lactose per minute at pH 4.5 at 30 ºC.

2.2. Gel beads preparation

Four different formulations were prepared, with the following composition: alginate (EA); alginate-trehalose (EAT); alginate-trehalose-guar gum (EATGG); alginate-trehalose-arabic gum (EATAG). All the solutions were prepared in 0.1 M acetate buffer pH 3.8. The final concentration of lactase solution was 0.775 mg/mL (slightly increased respect to Santagapita & Buera (2008b) in order to give good activity values with a relative small quantity of beads (9) for this encapsulation system). The enzyme and the initial solutions were carefully mixed for 2 min and maintained at 4 ± 1 ºC in order to avoid enzyme activity losses, minimizing the time employed between solution preparation and bead generation (around 10 min). Taking into account that the isoelectric point of the enzyme was 4.61 (Dashevsky, 1998) and the pk_a values of alginate are 3.38 and 3.65 (Santagapita, Mazzobre, & Buera, 2011), the buffer acetate at pH 3.8 was used in order to obtain an electrostatic interaction between the alginate (negatively charged) and the enzyme (positively charged). A

peristaltic pump was used to drop 10 mL of the alginate-enzyme mixture into 100 mL of the gelling solution, according to the drop method described by Austin, Bower and Muldoon (1996) with some modifications. Following the concentrations employed by Santagapita et al., 2011 and 2012, 1% (w/v) alginate solution containing enzyme was dropped into 2.5% (w/v) $CaCl_2$ solution (prepared in 0.1 M acetate buffer pH 3.8) for EA beads preparation. For EAT, EATGG and EATAG preparation, a 1% (w/v) alginate with 20% (w/v) trehalose and/or with 0.25% (w/v) of guar or arabic gums solutions containing the enzyme were dropped into the 2.5% (w/v) $CaCl_2$ solution supplemented with 20% (w/v) trehalose using the same procedure described previously. The 10 mL of each mixture were entirely dropped in 20 min.

$CaCl_2$ solution (with or without trehalose) was maintained in a cold bath with constant stirring (9.0 ± 0.1 rpm) and a needle with 0.25 mm diameter and 6 mm length (Novofine 32 G, Novo Nordisk A/S, Bagsvaerd, Denmark) was used for the dropping. The distance between the needle and the $CaCl_2$ solution was 6 cm. After beads generation, they were maintained 15 min in $CaCl_2$ solution (with constant stirring) and after that, there were washed 5 times with bidestilled cold water. The beads were placed on a blotting paper for 2 s, transferred to microcentrifuge tubes and were kept in refrigerator (to avoid enzymatic activity losses) until use.

2.3. Thermal Treatments

2.3.1. Freezing

Wet beads were frozen at -18ºC by using a conventional freezer during 24 h.

2.3.2. Freeze-drying

The beads were frozen as reported in 2.3.1. Freeze-drying (FD) was performed during 24 h in a Heto Holten A/S, cooling trap model CT 110 freeze-dryer (Heto Lab Equipment, Allerød, Denmark) operating at a condenser plate temperature of −110 °C and a minimum chamber pressure of $4 \cdot 10^{-4}$ mbar. The secondary drying was performed at 25 °C without shelf-control temperature.

2.3.3. Vacuum drying

Vacuum drying (VD) was carried out in a vacuum oven (Fistreem International Ltd, Loughborough, United Kingdom) at 25ºC and a pressure of 113 mbar during 24 h. Silica gel was used as desiccant agent.

After dehydration (by VD or FD), the beads were placed in microcentrifuge tubes and were kept in vacuum desiccators containing dried silica (in order to avoid further water uptake) until its determination.

2.4. β-Galactosidase activity

The enzyme activity was evaluated following the method described by Park, Santi, and Pastore (1979) with some modifications. 9 wet or dried beads were dissolved into 0.25 mL of 0.1 M citrate buffer pH 4.5 during 2 h at 4 ºC (without stirring, in order to avoid enzymatic activity losses). Subsequently, 0.25 mL of o-nitrophenyl-β-D-galactopyranoside (ONPG) (Sigma Chemical Co.) prepared in 0.1 M acetate buffer pH 3.8 was added and incubated during 15 min at 33 ºC. Finally, the reaction was stopped adding 0.5 mL of sodium carbonate 10% (w/v) and 1.75 mL of distilled water was added for subsequent measurement of o-nitrophenol (ONP) at 420 nm by using a Jasco V-630 UV-VIS spectrophotometer (JASCO Inc., Maryland, USA) at room temperature. Measurements were made in triplicate.

The remaining activity of the beads after thermal treatments was calculated as follows:

$$Remaining\ Activity\ (\%) = \frac{Activity_t}{Activity_0} \times 100 \quad (1)$$

Where $Activity_t$ is the activity value of each system obtained after a given treatment (freezing, freeze-drying or vacuum drying) and $Activity_0$ is related to the activity of the same system before the treatment (wet samples without treatment).

The loading efficiency of the enzyme in the beads after generation was determined through the loading efficiency parameter (L.E.) as follows:

$$Loading\ efficiency\ (\%) = \frac{L}{L_0} \times 100 \quad (2)$$

Where L is the amount of enzyme loaded in the beads after generation and L_0 is the initial amount of enzyme in the alginate solution.

2.5. Beads characterization

2.5.1. Digital image analysis

The size and shape of the beads were analysed through digital images captured by a digital camera coupled to a binocular microscope and analysed by the free license software ImageJ (http://rsbweb.nih.gov/ij/), as was described by Aguirre Calvo & Santagapita, (2016). The Feret's diameter (size) corresponds to the longest distance between any two points along the bead boundary. The circularity indicates how similar the bead is to a circle. At least 40 wet or dried beads of each system were analysed by applying the "analyse particle" command of the software. The ImageJ software was calibrated to transform the measured pixels in length units (mm) by taking pictures of a caliper section.

2.5.2. Water activity and water content

Water activity (a_w) of dried beads was determined by a dew point Hygrometer Decagon (Aqualab®, series 3 TE, Decagon Devices, Pullman, WA, USA). A special sample holder was used to reduce the quantity of beads needed. A calibration curve was performed with saturated salt solutions of known a_w (potassium acetate, potassium carbonate, sodium chloride and potassium chloride for a_w of 0.225, 0.432, 0.753, and 0.843, respectively -Greenspan, 1977-) and 1 (pure water). Measurements were made in triplicate.

Water content of the dried beads was obtained gravimetrically by the difference in weight before and after drying in vacuum oven for 48 h at 96 ± 2 ºC (Aguirre Calvo, & Santagapita, 2016). Water content determination was performed in duplicate.

2.6. Microstructure analysis by Scanning Electron Microscopy (SEM-FEG)

The morphology of dried beads was observed by a scanning electron microscopy with field emission gun (SEM-FEG) model supra 40 (Carl Zeiss SMT Inc., Peabody, MA, USA) with InLes detector. The sensitivity of the detector allowed to observed details in the beads structure without applying a metal cover to the samples. Beads were fixed to the SEM´s holder using double-sided adhesive tape. The magnifications used were 25000x and 200x at 1.00 kV.

2.7. Differential scanning calorimetry (DSC)

Glass transition temperature (T_g), the variations in heat capacity at T_g (Δcp) and the enthalpy relaxation of freeze-dried and vacuum dried beads were determined by differential scanning calorimetry (DSC) by means of a Mettler Toledo 822

equipment (Mettler Toledo AG, Urdorf, Switzerland) and STARe Thermal Analysis System version 8 software (Mettler Toledo AG). The instrument was calibrated using standard compounds (indium and zinc) of defined melting point and heat of melting.

All measurements were made in duplicate with 14-23 mg sample mass, using hermetically sealed aluminum pans of 40 μl inner volume (Mettler). Samples were heated from -100 to 100 ºC at 10 ºC/min under N_2 (flowed at 200 min/mL); an empty crucible was used as a reference. The reported data are the average of two determinations. After the first scan of the sample, a rescan of the same sample and at the same conditions was performed. The variations in heat capacity at T_g was reevaluated (Δcp of the rescan).

In order to analyze the enthalpy relaxation, the dried beads were aged at 25 °C during 37 days into hermetically sealed micro-centrifuge tubes. At the ageing temperature the samples were about 10-15 °C below T_g for trehalose-containing samples (Santagapita & Buera, 2008a). Glass transitions were recorded as the onset temperature of the discontinuities in the curves of heat-flow versus temperature (change in heat capacity).

2.8. Low Field Nuclear Magnetic Resonance (LF-NMR): isothermal studies

A Bruker Minispec mq20 (Bruker Biospin Gmbh, Rheinstetten, Germany) with a 0.47 T magnetic field operating at a resonance frequency of 20 MHz was used to study the transversal or spin–spin relaxation decay. The FID (free induction decay) sequence was used with the following setting: scans = 8, dummy shots = 0, recycle delay = 5 ms, gain = 81-83 dB. Wet beads equilibrated at 25.00 ± 0.01 °C in a thermal bath (Haake, model Phoenix II C35P, Thermo Electron Corporation Gmbh,

Karlsruhe, Germany) were measured at -20.05 °C ± 0.05, controlled by a BVT3000 unit (Bruker Biospin GmbH). Measurements were taken any 10 s during 10 min. The obtained signal (% solid component) is defined as the ratio of the signal from the solid component divided by the total NMR signal. This is based on the fact that the signal from the solid component decays very quickly, whereas the signal from the liquid component is preserved significantly longer. To account for the receiver dead time, the signal is extrapolated to t = 0 by multiplying with a correction factor called f-factor.

The Johnson–Mehl–Avrami–Kolmogorov equation (eq. 3) was used to fit the experimental data (Avrami, 1939; Buera et al., 2011; Dill, Folmer, & Martin, 2013; Johnson, & Mehl, 1939; Kolmogorov, 1937).

$$\alpha = 1 - \exp(-K_c t)^n \quad (3)$$

Where α is the solid crystal fraction obtained over time t; n is known as Avrami index, related to nucleation and dimension of crystal growing; and K_c [$(\text{time})^{-n}$], related to the isothermal crystallization rate (which mainly depends of temperature).

Data was normalized by the freezable water content, which was obtained by multiplying the fraction of the freezable water (x_{fw}, which were 0.86 for EA, 0.813 for EAT and 0.842 for EATAG and EATGG) with the water content (Traffano-Schiffo et al., 2017). Avrami parameters were obtained by fitting using Prism 6 (GraphPad Software Inc., San Diego, CA, USA). No constrains were imposed and, 0 and 1 were selected as initial values for K_c and n, respectively.

2.9. Statistical analysis

The effect of the treatments (freezing, FD and VD) and the composition on the measured parameters were analyzed by one-way ANOVA with Tukey`s post test by using Prism 6 (GraphPad Software Inc.). A *t* test was used to differentiate means of different treatments for the same system with 95 % of confidence between ($p< 0.05$).

3. Results and discussion

3.1. Effects of beads composition and drying on β-galactosidase activity preservation

High loading efficiencies were obtained, as expected, similar to those reported in literature to the same enzyme (Sen, Nath, Bhattacharjee, Chowdhury, & Bhattacharya, 2014) or different (invertase) (Santagapita et al., 2011) but using the same procedure. Alginate trehalose containing beads showed loading efficiencies of 92 ± 4 %, and the incorporation of guar or arabic gums lead to similar results (88 ± 8 %).

Figure 1 shows the remaining activity of lactase after freezing, freeze-drying and vacuum drying, where EA systems shows a remaining activity practically null after thermal treatments. The inclusion of trehalose was critical in order to stabilize the enzyme for all the applied treatments. According to the "water replacement theory", the conformation of the protein is maintained by the hydrogen bonds with the water. Upon freezing or drying, trehalose replaces the water establishing hydrogen bonds with the protein and therefore, stabilizing it. Also, the capacity of the sugar to generate a glassy matrix allows to immobilize the protein inside its matrix, reducing molecular movements and hereby avoiding protein denaturation (Grasmeijer, Stankovic, de Waard, Frijlink, & Hinrichs, 2013).

The addition of guar gum as a second excipient showed the highest remaining activity values for FD and VD (close to 95%) comparing with the other formulations. Similar results were obtained by Traffano-Schiffo et al. (2017) which showed that the presence of this gum also increases the remaining activity after 24 h of storage at 4 ºC and after four freeze/thaw cycles using liquid nitrogen. The conservative effect of guar gum in wet beads could be due to its high molecular mobility measured by LF-NMR, showing a high degree of rearrangement of the protons excipients inside the beads (Traffano-Schiffo et al., 2017), allowing a greater degree of interaction with the enzyme. In light of present results, it could be proposed that these interactions (mainly hydrogen bonds and van der Waals forces) were maintained during dehydration.

3.2. Effect of drying on physicochemical characteristics of beads

Water activity was determined for FD and VD beads. EA systems showed the higher a_w values, being 0.412 ± 0.004 and 0.386 ± 0.003 for FD and VD beads, respectively. a_w values obtained for trehalose-containing beads were between 0.365 and 0.392, where the lower values correspond to VD samples.

Table 1 shows the water content, the glass transition temperatures, the change in heat capacity at T_g (during the scan and rescan), and enthalpy relaxation (E.R.) for freeze-dried and vacuum dried beads.

The T_g value obtained for freeze-dried EA system was -24 ± 2 ºC, however, the T_g value of EA vacuum-dried beads could not be observed. Santagapita et al. (2012) were not able to obtain a T_g value for Ca(II)-alginate beads containing invertase. In

contrast, the glass transitions temperatures for beads containing trehalose were significantly higher than EA, reaching values between 35 and 40 ºC for all the studied treatments. These high T_g values indicate that the trehalose-containing beads were in the glassy state at ambient temperature, stabilizing the enzyme as observed in Figure 1, and assuring stability as long as temperature or humidity did not increase. Similar T_g values for trehalose containing beads were previously reported (Santagapita et al., 2012; Santagapita & Buera, 2008a).

The significant higher Δcp values associated to T_g obtained for trehalose containing beads than for EA beads is consistent with fact that sugars depict transitions with higher Δcp values than polymers, which also developed the transition in a longer range of temperatures, being more difficult to be observed (Santagapita et al., 2012; Katayama et al., 2008). Among the trehalose-containing beads, no significant differences were observed by the addition of guar or arabic gums, revealing that trehalose is the main contributor to the generation of the amorphous matrix.

Being the T_g a reversible transition, the Δcp values after the rescan can be interpreted as the capacity of the matrix to regenerate the glassy state from the supercooled state after the first scan. According to the data of Table 1, no significant differences were obtained among the drying treatments, showing similar capacity of recovery.

Enthalpy relaxation is an important characteristic of the amorphous materials, and is often observed as an endothermic event within the T_g region during heating (Santagapita, & Buera, 2008a). Since glassy materials are thermodynamically unstable, their structure could relax towards the equilibrium state during storage above T_g, being it extent also a function of temperature and time (Santagapita, & Buera, 2008a). Beads containing trehalose were aged during 37 days between 10 and

15 °C below their T_g value prior DSC analysis. No significant differences were obtained between VD and FD treatments for each type of beads. Besides, FD beads showed similar stability among the different systems. Among the VD beads, the presence of guar gum produced glassy matrices of higher enthalpy values than the others trehalose-containing beads, indicating a key role in the matrix formation, which in turn could favor the enzyme activity conservation. Higher relaxation enthalpy values were linked to higher remaining activity conservation in lactase-trehalose model systems (Santagapita & Buera, 2008a). A higher relaxation enthalpy value corresponds to a more perfect glass, represented by an extended glassy region formed during ageing.

Figure 2 shows the images obtained by SEM for freeze and vacuum dried beads. As can be seen in the images on the left side of each treatment (200x), freeze-dried beads had more spongy and voluminous surface, while the vacuum dried beads were more compact and showed less exposed surface area compared with FD samples. At higher magnifications (25000x) big differences in the surface of the beads can be appreciated: the beads subjected to VD showed large cracks, as a result of its breakable surface, and also consistent with the high size reduction of the beads. However, this structural characteristic did not affect the enzyme remaining activity (Figure 1). All trehalose-containing beads showed the typical glassy structure, which is supported by the DSC analysis showed in Table 1. Instead, EA beads showed the typical structure of supercooled liquid, showing a less smooth surface, as result of the lower viscosity of the supercooled liquid respect to the glassy state.

In order to characterize the beads according to its size and shape, Feret´s diameter and circularity were obtained (Figure 3). Figure 3a shows the Feret´s diameter of wet

(after generation) and dried beads (FD and VD) with different composition. Wet beads showed a Feret's diameter close to 1.5 mm, similar to the one reported in other works (Santagapita et al., 2012; Traffano-Schiffo et al., 2017), showing significant increments by the addition of gums, as previously reported (Traffano-Schiffo et al., 2017). VD beads showed significant smaller Feret´s diameter comparing with FD and wet beads, reaching values close to 1 mm (Feret´s diameter below 1.08 ± 0.09 mm). It is important to highlight that the addition of trehalose significantly incremented the beads size respect to alginate beads for each drying treatment. In addition, the presence of gums further increased the size respect to trehalose-containing beads, especially in FD beads. These facts are linked to the raise in viscosity produced by the addition of guar gum, and to the modification in the interfacial properties (protein-polysaccharide structure) caused by arabic gum (Busch et al., 2017). Guar gum inclusion even avoided the size reduction in FD beads, which could have interesting technological implications.

Figure 3b shows the circularity of the beads, where trehalose containing beads subjected to VD treatment showed a significant higher circularity value close to 0.8 and FD beads showed much lower circularity values (between 0.5 and 0.6). These results are consistent with the FEG-SEM images previously discussed (Figure 2) and it could be explained from the physic point of view of the applied drying treatments. During VD, the beads contract due to the evaporation of the water molecules, reducing its volume. In contrast, during the sublimation step, large pores are formed on the FD beads. These pores correspond to the spaces previously occupied by ice crystals, showing as a consequence a spongy surface of higher volume. In addition,

the contraction of the VD beads could also explain the presence of the cracks observed in FEG-SEM images.

3.3. Isothermal crystallization by LF-NMR

In a previous work, Traffano-Schiffo and co-workers (2017) observed that the presence of gums increased the onset temperatures of ice melting (T_m') determined by DSC in Ca(II)-alginate beads containing trehalose. Besides, these beads depicted T_g values around-65 °C. However, neither of these parameters were adequate predictors of the remaining activity of the enzyme in beads. In order to deeply understand the results obtained by freezing Ca(II)-alginate beads, LF-NMR studies were conducted.

Figure 4 shows the increment of the solid fraction on wet beads isothermally treated at -20 °C. The measurement relays on the different relaxation times between the protons belonging to liquid and solid phases. Typically, wet beads depicted two mobile protons populations between 54-66 ms and 379-710 ms, respectively (Traffano-Schiffo et al., 2017). When a solid fraction is generated, a much shorter T_2 is observed. By relating the T_2 from both solid and total (solid plus liquid) contributions, it is possible to study the increment of the solid fraction at subzero temperatures from wet beads due to ice crystallization.

Considering that T_m´ of the beads systems lies between -8 and -2 °C and T_g around -64/65 °C (for trehalose containing beads) (Traffano-Schiffo et al., 2017), ice crystallization will be the main phenomenon produced at -20 °C. Figure 4a shows the unprocessed data of the solid fraction on wet beads. It is clearly observed that EA samples achieved complete ice crystallization. Instead, in trehalose containing

samples only 80% of the solid fraction was achieved. The final solid percentage at which each sample finally stabilizes at -20 °C follows the same trend of unfreezable water present in each system obtained by DSC data (Traffano-Schiffo et al., 2017).

JMAK equation (Avrami, 1939; Johnson, & Mehl, 1939; Kolmogorov, 1937) was used to fit the experimental data. Two parameters are derived: *n*, which gives information about nucleation and dimension of crystal growing; and K_c, related to the isothermal crystallization rate. The model implies that the crystallization starts randomly at different points and it propagates from each nucleation point (Gedde, 1995). Avrami equation only adequately fitted EA samples in Figure 4a, following sigmoidal crystallization kinetics, with an *n* value of 2.03 ± 0.07. This implies that the dimension of crystal growing is bidimensional. Xu and co-workers (2016) obtained a $n \sim 1$ by studying amorphous solid water films, even though their experiment involved grow from a well-defined interface, while the model assumes randomly nucleation points. However, they observed a sigmoideal crystallization kinetics, typical from a nucleation and growth process, such as the one observed here. It is already known that alginate can retard the rate of ice-crystal growth in ice creams (Nussinovitch, 1997) by increasing viscosity or by quelating Ca(II). Besides, Gryshkov, Pogozhykh, Hofmann, Mueller and Glasmacher (2014) employed Ca(II)-alginate beads for cryopreservation purposes, thinking that gel-like structures and mild environment inside alginate beads could resist the reorganization of ice crystals during thawing, minimizing cell damage. However, to the best of our knowledge, for the first time ice crystallization kinetics inside Ca(II)-alginate beads were obtained through LF-NMR.

Figure 4b shows the normalized solid fraction for comparison of the crystal growing of the four beads systems. It is clearly see that ice crystallization in Ca(II)-alginate beads followed the so called Avrami kinetics of nucleation and growth. The fitting of the curves was acceptable as observed in Figure 4b, aside from the goodness of the fit, which also showed very good values (the R^2 were between 0.9983 and 0.9927). It is known that the JMAK equation predicts correctly the real transformed fraction only if the number of the growing nuclei in the controlled volume is large (Todinov, 2000) and if they are randomly oriented and with low anisotropy degree (Levine, Narayan, and Kelton, 1997). The fitting of the presented data was accepted in the whole range of solid content, considering that the deviation of all the curves was small and similar. Figure 4b shows that the inclusion of trehalose or gums did not affect the dimension of the ice growing (= n) nor its rate (= K_c). Then, it is possible to conclude that the main effect on enzyme stability is the generation of glassy matrix during freezing, with the concomitant reduction of crystallized water. There was not effect of trehalose or gums on ice crystallization inside beads, leaving unaffected kinetics rate, nucleation and growing. It was proved that the addition of a second excipient to sugar or polyol matrices designed for protecting biomolecules (in pharmaceutical or food-ingredient formulations) can be beneficial. Buera, Schebor and Elizalde, (2005) showed that the presence of proteins retarded sugar crystallization, and in parallel, sugars retarded protein denaturation. There is also evidence that the presence of polymers or salts produced inhibition of trehalose crystallization (Mazzobre, Santagapita, Gutiérrez, Buera, 2008, Santagapita, & Buera, 2008a). However, these effects were not observed for ice crystallization in Ca(II)-alginate beads.

4. Conclusions

Trehalose was critical for β-galactosidase conservation in Ca(II)-alginate beads after drying treatments. Guar gum as a second excipient showed the higher conservation effect for both treatments.

Trehalose was the main responsible of the formation of an amorphous matrix in the beads, showing T_g values close to 40 ºC, assuring very stable systems at ambient temperature. The presence of guar gum produced glassy matrices of high enthalpy values for both types of drying, indicating a key role in the matrix formation and, in turn, in enzyme activity conservation.

According to the size and morphology, VD beads showed smaller size and higher circularity comparing with FD and wet beads. The presence of trehalose significantly incremented the size respect alginate beads for both drying treatments. Besides, gums further increased the size, especially in FD beads. FEG-SEM images have revealed that FD beads had more spongy and voluminous surface, while VD beads showed large cracks (breakable surface). All trehalose-containing beads showed the typical glassy structure, which was supported by the DSC analysis.

For the first time, an isothermal crystallization analysis of Ca(II)-alginate beads containing β-galactosidase was carried out by LF-NMR. It revealed that the ice crystallization inside the beads follows the Avrami kinetics of nucleation and growth. The final ice fraction obtained was in agreement with the freezable water obtained by DSC.

The results of this research open an opportunity in the design and development of new lactose-containing foods able to be consumed by lactose intolerance people.

5. Acknowledgements

This work was supported by Universidad de Buenos Aires (UBACyT 20020130100610BA), Agencia Nacional de Promoción Científica y Tecnológica (ANPCyT PICT 2013 0434 and 2013 1331), CIN-CONICET (PDTS 2015 n° 196), and Consejo Nacional de Investigaciones Científicas y Técnicas.

The author María Victoria Traffano Schiffo wants to thank "Programa para la Formación de Personal Investigador (FPI)" Pre-doctoral Program of the Universitat Politècnica de València (UPV) for support her PhD studies and also her mobility to Argentina.

6. References

Aguirre Calvo, T. R., Busch, V. M., & Santagapita, P. R. (2017). Stability and release of an encapsulated solvent-free lycopene extract in alginate-based beads. *LWT-Food Science and Technology*, 77, 406-412.

Aguirre Calvo, T., & Santagapita, P. (2016). Physicochemical characterization of alginate beads containing sugars and biopolymers. *Journal of Quality and Reliability Engineering*, 2016.

Austin, L., Bower, J. J., & Muldoon, C. (1996). The controlled release of leukaemia inhibitory factor (LIF) from gels. *Proceeding of the International Symposium on Controlled Release of Bioactive Materials*, 23, 739-740.

Avrami, M. (1939). Kinetics of phase change. I General theory. *The Journal of Chemical Physics*, 7(12), 1103-1112.

Buera, M. P., Roos, Y., Levine, H., Slade, L., Corti, H. R., Reid, D. S., ... & Angell, C. A. (2011). State diagrams for improving processing and storage of foods, biological materials, and pharmaceuticals (IUPAC Technical Report). *Pure and Applied Chemistry*, 83(8), 1567-1617.

Buera, M. P., Schebor, C., & Elizalde, B. (2005). Effects of carbohydrate crystallization on stability of dehydrated foods and ingredient formulations. *Journal of Food Engineering*, 67(1), 157-165.

Busch, V. M., Pereyra-Gonzalez, A., Šegatin, N., Santagapita, P. R., Ulrih, N. P., & Buera, M. P. (2017). Propolis encapsulation by spray drying: characterization and stability. *LWT-Food Science and Technology*, 75, 227-235.

Dashevsky, A. (1998). Protein loss by the microencapsulation of an enzyme (lactase) in alginate beads. *International Journal of Pharmaceutics*, 161(1), 1-5.

De Santis, F., Pantani, R., & Titomanlio, G. (2011). Nucleation and crystallization kinetics of poly (lactic acid). *Thermochimica Acta*, 522(1), 128-134.

Dill, E. D., Folmer, J. C., & Martin, J. D. (2013). Crystal growth simulations to establish physically relevant kinetic parameters from the empirical Kolmogorov–Johnson–Mehl–Avrami model. *Chemistry of Materials*, 25(20), 3941-3951.

Estevinho, B. N., Ramos, I., & Rocha, F. (2015). Effect of the pH in the formation of β-galactosidase microparticles produced by a spray-drying process. *International Journal of Biological Macromolecules*, 78, 238-242.

Furlán, L. T. R., Baracco, Y., Lecot, J., Zaritzky, N., & Campderrós, M. E. (2017). Effect of sweetener combination and storage temperature on physicochemical properties of sucrose free white chocolate. *Food Chemistry*, 229, 610-620.

Gedde, W.U. (1995). Crystallization kinetics. In U.W. Gedde (Ed.), *Polymer Physics* (pp. 169-198). London: Springer.

Grasmeijer, N., Stankovic, M., de Waard, H., Frijlink, H. W., & Hinrichs, W. L. (2013). Unraveling protein stabilization mechanisms: vitrification and water replacement in a glass transition temperature controlled system. *Biochimica et Biophysica Acta (BBA)-Proteins and Proteomics*, 1834(4), 763-769.

Greenspan, L. (1977). Humidity fixed points of binary saturated aqueous solutions. Journal of Research of the National Bureau of Standards, 81(1), 89-96.

Gryshkov, O., Pogozhykh, D., Hofmann, N., Mueller, T., & Glasmacher, B. (2014). C-1009: Cryopreservation of monkey mesenchymal stem cells inside alginate 3D micro-spheres after a high voltage encapsulation. *Cryobiology*, 69(3), 514.

He, X., Liu, Y., Li, H., & Li, H. (2016). Single-stranded structure of alginate and its conformation evolvement after an interaction with calcium ions as revealed by electron microscopy. *RSC Advances*, 6(115), 114779-114782.

Heaney, R. P. (2013). Dairy intake, dietary adequacy, and lactose intolerance. *Advances in Nutrition: An International Review Journal*, 4(2), 151-156.

Johnson, W. A., & Mehl, R. F. (1939). Reaction kinetics in processes of nucleation and growth. *Trans. Aime,* 135(8), 396-415.

Katayama, D. S., Carpenter, J. F., Manning, M. C., Randolph, T. W., Setlow, P., & Menard, K. P. (2008). Characterization of amorphous solids with weak glass transitions using high ramp rate differential scanning calorimetry. *Journal of Pharmaceutical Sciences*, 97(2), 1013-1024.

Kolmogorov, A. N. (1937). On the statistical theory of the crystallization of metals. *Bulletin of the Russian Academy of Science.*1, 355-359.

Lee, K. Y., & Mooney, D. J. (2012). Alginate: properties and biomedical applications. *Progress in Polymer Science*, 37(1), 106-126.

Levine, L. E., Lakshmi Narayan, K., & Kelton, K. F. (1997). Finite size corrections for the Johnson–Mehl–Avrami–Kolmogorov equation. *Journal of Material Research*, 12, 124-132.

Mazzobre, M. F., Aguilera, J. M., & Buera, M. P. (2003). Microscopy and calorimetry as complementary techniques to analyze sugar crystallization from amorphous systems. *Carbohydrate Research*, 338(6), 541-548.

Mazzobre, M. F., Longinotti, M. P., Corti, H. R., & Buera, M. P. (2002). Effect of salts on the properties of aqueous sugar systems, in relation to biomaterial stabilization. 1. Water sorption behavior and ice crystallization/melting. *Cryobiology*, 43(3), 199-210.

Mazzobre, M. F., Santagapita, P. R., Gutiérrez, N., & Buera, M. P. (2008). Consequences of matrix structural changes on functional stability of enzymes as affected by electrolytes. In G. Gutiérrez-López, G. Barbosa-Cánovas, J. Welti-Chanes, & E. Parada-Arias (Eds.), *Food Engineering: Integrated Approaches* (pp. 73–87). New York: Springer.

Misselwitz, B., Pohl, D., Frühauf, H., Fried, M., Vavricka, S. R., & Fox, M. (2013). Lactose malabsorption and intolerance: pathogenesis, diagnosis and treatment. *United European Gastroenterology Journal*, 1(3), 151-159.

Nussinovitch, A. (1997). Hydrocolloid applications: gum technology in the food and other industries. In A. Nussinovitch (Ed.), *Alginates* (pp. 19-39). London: Chapman & Hall.

Park, Y. K., Santi, M. S. S., & Pastore, G. M. (1979). Production and characterization of β-galactosidase from *Aspergillus oryzae*. *Journal of Food Science*, 44(1), 100-103.

Santagapita, P. R., & Buera, M. P. (2008a). Electrolyte effects on amorphous and supercooled sugar systems. *Journal of Non-Crystalline Solids*, 354(15), 1760-1767.

Santagapita, P. R., & Buera, M. P. (2008b). Trehalose–water–salt interactions related to the stability of β-galactosidase in supercooled media. *Food Biophysics*, 3(1), 87-93.

Santagapita, P. R., Mazzobre, M. F., & Buera, M. P. (2011). Formulation and drying of alginate beads for controlled release and stabilization of invertase. *Biomacromolecules*, 12(9), 3147-3155.

Santagapita, P. R., Mazzobre, M. F., & Buera, M. P. (2012). Invertase stability in alginate beads: effect of trehalose and chitosan inclusion and of drying methods. *Food Research International*, 47(2), 321-330.

Sen, P., Nath, A., Bhattacharjee, C., Chowdhury, R., & Bhattacharya, P. (2014). Process engineering studies of free and micro-encapsulated β-galactosidase in batch and packed bed bioreactors for production of galactooligosaccharides. *Biochemical Engineering Journal*, 90, 59-72.

Todinov, M. T. (2000). On some limitations of the Johnson–Mehl–Avrami–Kolmogorov equation. *Acta Materialia*, 48, 4217–4224.

Traffano-Schiffo, M. V., Aguirre Calvo, T. R., Castro-Giraldez, M., Fito, P. J. & Santagapita, P. R. (2017). Alginate beads containing lactase: stability and microstructure. *Biomacromolecules*, 18, 1785-1792.

Tsai, F. H., Chiang, P. Y., Kitamura, Y., Kokawa, M., & Islam, M. Z. (2017). Producing liquid-core hydrogel beads by reverse spherification: Effect of secondary gelation on physical properties and release characteristics. *Food Hydrocolloids*, 62, 140-148.

Vasile, F. E., Romero, A. M., Judis, M. A., & Mazzobre, M. F. (2016). *Prosopis alba* exudate gum as excipient for improving fish oil stability in alginate–chitosan beads. *Food Chemistry*, 190, 1093-1101.

Wahba, M. I. (2016). Treated calcium pectinate beads for the covalent immobilization of β-d-galactosidase. *International Journal of Biological Macromolecules*, 91, 877-886.

Wu, Z., Wang, Z., Guan, B., Wang, X., Zhang, Y., Xiao, Y., Zhi, B., Liu, Y., Li, Z., & Huo, Q. (2013). Improving the properties of β-galactosidase from *Aspergillus oryzae* via encapsulation in aggregated silica nanoparticles. *New Journal of Chemistry*, 37(11), 3793-3797.

Xu, Y., Petrik, N. G., Smith, R. S., Kay, B. D., & Kimmel, G. A. (2016). Growth rate of crystalline ice and the diffusivity of supercooled water from 126 to 262 K. *Proceedings of the National Academy of Sciences*, 113(52), 14921-14925.

Zeeb, B., Saberi, A. H., Weiss, J., & McClements, D. J. (2015). Formation and characterization of filled hydrogel beads based on calcium alginate: factors influencing nanoemulsion retention and release. *Food Hydrocolloids*, 50, 27-36.

Zhang, Z., Zhang, R., & McClements, D. J. (2017). Lactase (β-galactosidase) encapsulation in hydrogel beads with controlled internal pH microenvironments: Impact of bead characteristics on enzyme activity. *Food Hydrocolloids*, 67, 85-93.

Zhang, Z., Zhang, R., Zou, L., & McClements, D. J. (2016). Protein encapsulation in alginate hydrogel beads: Effect of pH on microgel stability, protein retention and protein release. *Food Hydrocolloids*, 58, 308-315.

Table 1. Water content (X_w, on dry basis), glass transition temperature (T_g), change in heat capacity at T_g (Δcp), enthalpy relaxation (E.R.) and the change in heat capacity (Δcp) during the rescan were obtained for freeze-dried (FD) and vacuum dried (VD) beads by DSC. E: enzyme; A: alginate; T: trehalose; AG: arabic gum; GG: guar gum. Standard deviation values are included.

Treatment	Systems	Glass Transition		E. R. (J/g)	Δcp^{rescan}(J/gK)	X_w (kg_w/kg_{db})
		T_g (ºC)	Δcp (J/gK)			
FD	EA	-24 ± 2^{b}	0.11 ± 0.08^{b}	-	-	0.1810 ± 0.0006^{a}
	EAT	40 ± 2^{a}	0.63 ± 0.04^{a}	-2.3 ± 0.7^{a}	0.2 ± 0.2^{a}	0.079 ± 0.009^{b}
	EATAG	37 ± 5^{a}	$0.37 \pm 0.04^{a*}$	-3.3 ± 0.3^{a}	$0.147 \pm 0.007^{a*}$	0.069 ± 0.002^{b}
	EATGG	40.4 ± 0.1^{a}	0.6 ± 0.1^{a}	-2 ± 1^{a}	0.27 ± 0.01^{a}	0.07 ± 0.01^{b}
VD	EA	-	-	-	-	0.19 ± 0.01^{a}
	EAT	35.7 ± 0.1^{b}	0.71 ± 0.05^{a}	-0.3 ± 0.2^{b}	0.46 ± 0.08^{a}	0.088 ± 0.003^{b}
	EATAG	37.60 ± 0.08^{ab}	$0.65 \pm 0.02^{a*}$	-1.17 ± 0.07^{b}	$0.45 \pm 0.03^{a*}$	0.082 ± 0.003^{b}
	EATGG	38.1 ± 0.9^{a}	0.5 ± 0.1^{a}	-2.3 ± 0.4^{a}	0.40 ± 0.08^{a}	0.083 ± 0.004^{b}

$^{a-b}$ Different letters on the columns indicate significant differences between means of the same treatment; * indicate significant differences between means of the same system ($p < 0.05$).

Caption for Figures

Figure 1. Remaining activity of lactase (%) after thermal treatments: freezing (24 h at -18 ºC); freeze-drying (FD) and vacuum drying (VD). E: enzyme; A: alginate; T: trehalose; AG: arabic gum; GG: guar gum. For a certain treatment bars with the same letter (a-c) indicate no significant differences ($p < 0.05$); for beads of same composition bars with the same number have no significant differences between treatments ($p < 0.05$).

Figure 2. Images obtained in a scanning electron microscope (SEM) of freeze-drying (FD) and vacuum-drying (VD) beads at two different magnifications. E: enzyme; A: alginate; T: trehalose; AG: arabic gum; GG: guar gum.

Figure 3. a) Feret´s diameter and b) circularity of wet, freeze-dried (FD) and vacuum dried (VD) beads with different composition. E: enzyme; A: alginate; T: trehalose; AG: arabic gum; GG: guar gum. For a certain treatment bars with the same letter (a-d) indicate no significant differences ($p < 0.05$); for beads of same composition bars with the same number (1-3) have no significant differences between treatments ($p < 0.05$).

Figure 4. Isothermal LF-NMR: solid fraction vs time at -20 °C. a) raw data (solid fraction) and b) normalized solids by freezable water content. Experimental data (symbols) were fitted using Avrami equation (lines).

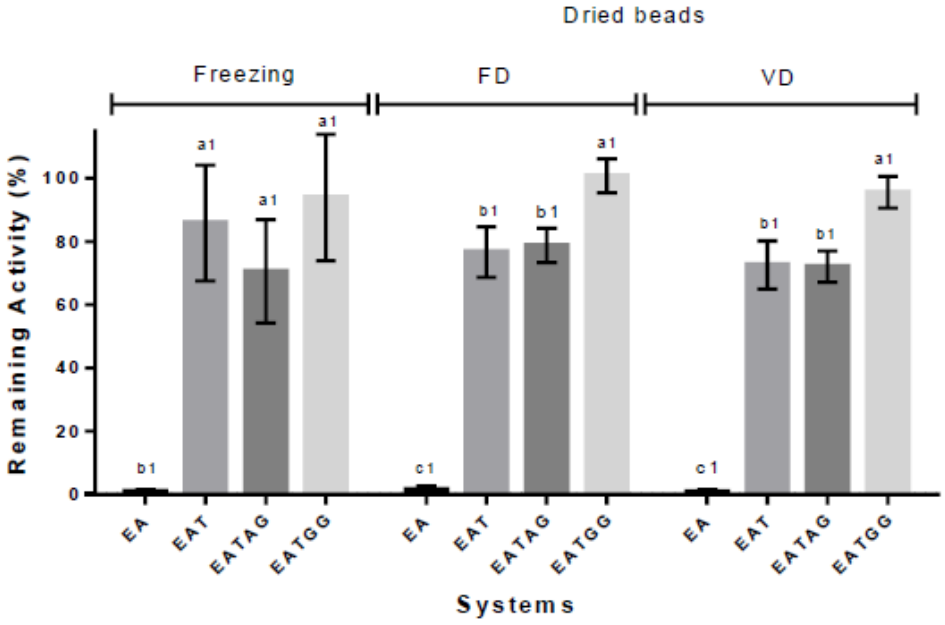

Figure 1.

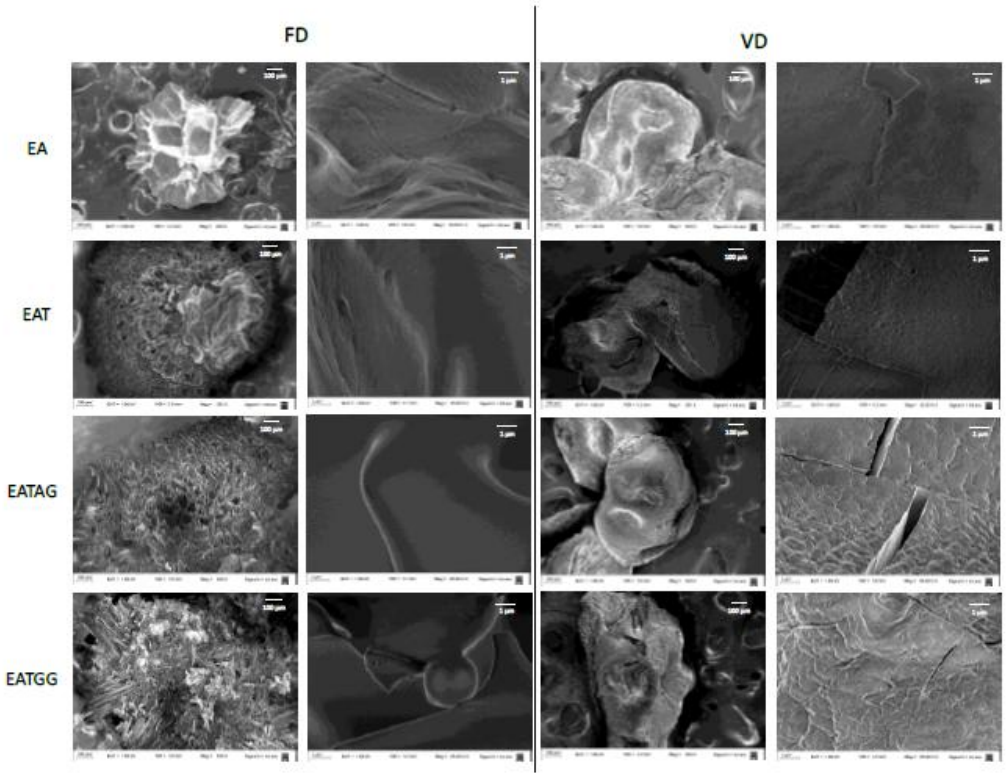

Figure 2.

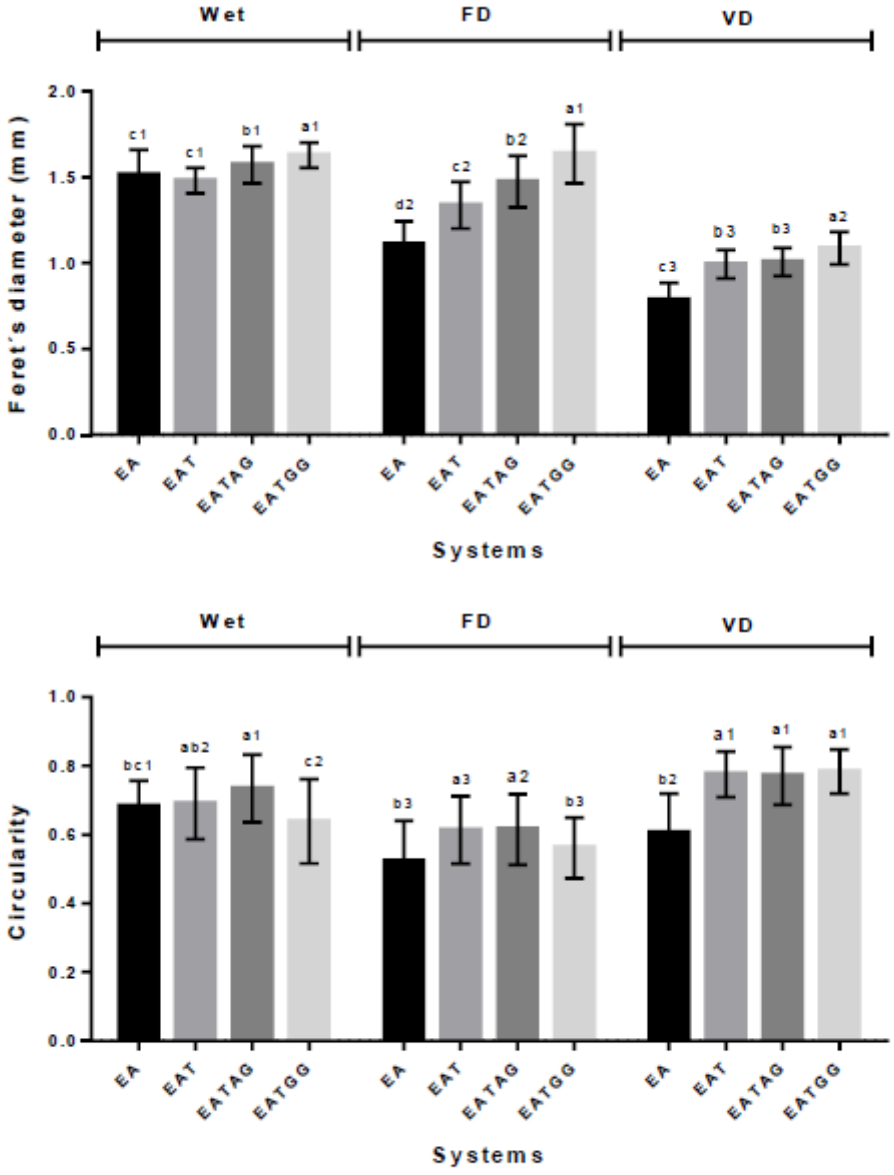

Figure 3.

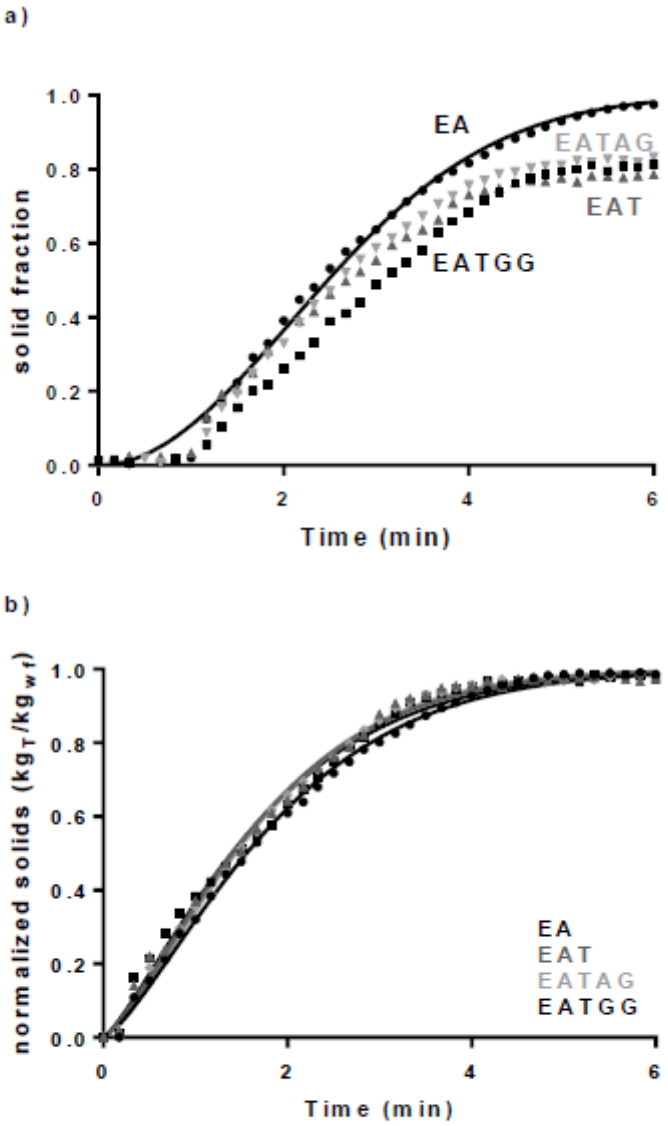

Figure 4.

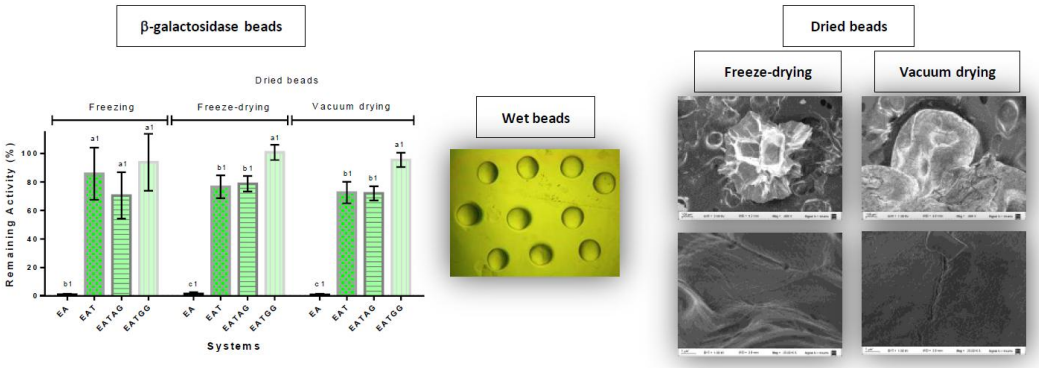

Graphical Abstract

RESEARCH HIGHLIGHTS

- Lactase encapsulated in alginate-Ca(II) beads was successfully dried by two methods
- Beads with trehalose and guar gum showed the higher conservation effect
- T_g values of trehalose-containing beads wasclose to 40 ºC, assuring stable systems
- Vacuum dried beads showed smaller size and higher circularity than freeze-dried ones
- Ice crystallization inside the beads analyzed by LF-NMR follows Avrami kinetics